Eur. Phys. J. A **25**, s01, 493–498 (2005)
DOI: 10.1140/epjad/i2005-06-136-7

EPJ A direct
electronic only

Shell-model description of weakly bound and unbound nuclear states

N. Michel[1,2,3,a], W. Nazarewicz[1,2,4], M. Płoszajczak[5,b], and J. Rotureau[5]

[1] Department of Physics and Astronomy, University of Tennessee, Knoxville, TN 37996, USA
[2] Physics Division, Oak Ridge National Laboratory, P.O. Box 2008, Oak Ridge, TN 37831, USA
[3] Joint Institute for Heavy Ion Research, Oak Ridge, TN 37831, USA
[4] Institute of Theoretical Physics, Warsaw University, ul. Hoża 69, 00-681 Warsaw, Poland
[5] Grand Accélérateur National d'Ions Lourds (GANIL), CEA/DSM-CNRS/IN2P3, BP 55027, F-14076 Caen Cedex 05, France

Received: 20 March 2005 /
Published online: 8 July 2005 –

Abstract. A consistent description of weakly bound and unbound nuclei requires an accurate description of the particle continuum properties when carrying out multiconfiguration mixing. This is the domain of the Gamow Shell Model (GSM) which is the multiconfigurational shell model in the complex k-plane formulated using a complete Berggren ensemble representing bound single-particle (s.p.) states, s.p. resonances, and non-resonant complex energy continuum states. We shall discuss the salient features of effective interactions in weakly bound systems and show selected applications of the GSM formalism to p-shell nuclei. Finally, a development of the new non-perturbative scheme based on Density Matrix Renormalization Group methods to select the most significant continuum configurations in GSM calculations will be discussed shortly.

PACS. 21.60.Cs Shell model – 24.10.Cn Many-body theory – 27.20.+n Properties of specific nuclei listed by mass ranges: $6 \leq A \leq 19$

1 Introduction

The binding of nuclei close to the particle drip lines depends sensitively both on the coupling to scattering states and on the effective *in-medium* NN interaction which itself is modified by the continuum coupling [1]. Weakly bound nuclei are best described in the open quantum system formalism allowing for configuration mixing, such as the real-energy continuum shell model (see ref. [2] for a recent review) and, most recently, the complex-energy continuum Gamow Shell Model (GSM) [3,4,5,6,7] (see also refs. [8,9]). GSM is the multi-configurational shell model with a single-particle (s.p.) basis given by the Berggren ensemble [10] which consists of Gamow (or resonant) states and the complex non-resonant continuum. The s.p. Berggren basis is generated by a finite-depth potential, and the many-body states are obtained in shell-model calculations as the linear combination of Slater determinants spanned by resonant and non-resonant s.p. states. Hence, both continuum effects and correlations between nucleons are taken into account simultaneously. All details of the formalism can be found in refs. [4,5], in which the GSM was applied to many-neutron configurations in neutron-rich helium, oxygen, and lithium isotopes.

Even though the effective interaction theory for open quantum many-body systems has not yet been developed (see, however, recent attempts in ref. [11]), recent investigations [12,13] in the framework of the Shell Model Embedded in the Continuum (SMEC) [14,2] established basic features of the correction to the eigenenergy of the closed quantum system due to the continuum coupling. The novel feature, absent in the standard SM, is a strong influence of the poles of the scattering (S) matrix on the weakly bound/unbound states. In particular, for nucleons in low-ℓ orbits ($\ell = 0, 1$), the coupling becomes singular at the particle emission threshold if the pole of the S-matrix lies at the threshold [12,13]. Such a coupling may induce the non-perturbative rearrangement of the wave function. Below, we shall illustrate this effect in the case of spectroscopic factors of 0^+ states in ^{6}He.

2 Average spherical Gamow-Hartree-Fock potential

In earlier studies [3,4], we have used the s.p. basis generated by a Woods-Saxon (WS) potential which was adjusted to reproduce the s.p. energies in ^{5}He ("^{5}He" parameter set [4]). This "^{5}He" WS basis is unsuitable when applied to the neutron-rich helium isotopes. Therefore, we use an optimized Berggren basis given by the Hartree-Fock (HF) method extended to unbound states (the so-called

[a] e-mail: michel@ler000.phy.ornl.gov
[b] Conference presenter; e-mail: ploszajczak@ganil.fr

Gamow-Hartree-Fock (GHF) approach). This allows for a more precise description of heavier p-shell nuclei in the GSM calculations [5].

The spherical HF potential cannot be defined for open-shell nuclei and one has to resort to approximations. The first ansatz is the usual uniform-filling approximation in which HF occupations are averaged over all magnetic substates of an individual spherical shell. In the second ansatz, the deformed HF potential corresponding to non-zero angular momentum projection is averaged over all the magnetic quantum numbers (the so-called M-potential). For closed-shell nuclei, both methods yield the true HF potential.

To define the M-potential, one occupies the s.p. states in the valence shell that have the largest angular momentum projections on the third axis. The resulting Slater determinant corresponds to the angular momentum $J = M$. For closed-shell nuclei ($M = 0$) and for nuclei with one particle (or hole) outside a closed subshell ($M = j$), this Slater determinant can be associated with the ground state (g.s.) of the s.p. Hamiltonian. Spherical M-potential, U_M, is defined by averaging the resulting HF potential over magnetic quantum number m:

$$\langle\alpha|U_M|\beta\rangle = \langle\alpha|\hat{h}|\beta\rangle + \frac{1}{N_{l,j}} \sum_{m=j+1-N_{l,j}}^{j} \sum_{\lambda} \langle\alpha m\, \lambda m_\lambda|\hat{V}|\beta m\, \lambda m_\lambda\rangle, \quad (1)$$

where $\hat{h}$ is the s.p. Hamiltonian (given by a WS+Coulomb potential), λ is an occupied shell with angular quantum numbers (j_λ, l_λ), $N(\lambda)$ is the number of nucleons occupying this shell, and $\hat{V}$ is the residual shell-model interaction. In the above expression, $N_{l,j}$ is the number of nucleons occupying the valence shell with quantum numbers l, j.

While the HF procedure is well defined for the bound states, it has to be modified for the unbound s.p. states (resonant or scattering), even in the case of closed-shell nuclei. First, the effective nuclear two-body interaction has to be quickly vanishing beyond a certain radius; otherwise the resulting HF potential diverges, thus providing incorrect s.p. asymptotics. Moreover, as resonant states are complex, the resulting self-consistent HF potential is complex as well. This is to be avoided, as the Berggren completeness relation assumes a real potential. Therefore, we take the real part of the GHF potential to generate the s.p. basis.

3 Description of the Gamow Shell Model calculation

3.1 Choice of the average potential, the Hamiltonian and the valence space

For the residual interaction, we take a finite-range Surface Gaussian Interaction (SGI) [7]:

$$V_{J,T}(\mathbf{r}_1, \mathbf{r}_2) = V_0(J,T) \cdot \exp\left[-\left(\frac{\mathbf{r}_1 - \mathbf{r}_2}{\mu}\right)^2\right] \cdot \delta(|\mathbf{r}_1| + |\mathbf{r}_2| - 2 \cdot R_0), \quad (2)$$

which is used, together with the WS potential with the "^{5}He" parameter set, to generate an optimal GHF basis. The Hamiltonian employed can thus be written as: $\hat{H} = \hat{H}^{(1)} + \hat{H}^{(2)}$, where $\hat{H}^{(1)}$ is the one-body Hamiltonian described above augmented by a hard sphere Coulomb potential of radius R_0 (corresponding to the ^{4}He core), and $\hat{H}^{(2)}$ is the two-body interaction among valence particles, which can be written as a sum of SGI and Coulomb terms. The Coulomb two-body matrix elements are calculated using the exterior complex scaling as described in ref. [4] and can be treated as precisely as nuclear terms.

The principal advantage of the SGI is that it is finite-range, so no energy cutoff is needed. Moreover, the surface delta term simplifies the calculation of two-body matrix elements, because they can be reduced to one-dimensional radial integrals. Consequently, a local adjustment of the Hamiltonian parameters in GSM/GHF calculations becomes feasible.

In this chapter, the valence space for protons and neutrons consists of the $0p_{3/2}$ and $0p_{1/2}$ GHF resonant states, calculated for each nucleus, and the $\{ip_{3/2}\}$ and $\{ip_{1/2}\}$ $(i = 1, \cdots, n)$ complex and real continua generated by the same potential. These continua extend from $\Re[k] = 0$ to $\Re[k] = 8\,\mathrm{fm}^{-1}$, and they are discretized with 14 points (*i.e.*, $n = 14$). The $0p_{1/2}$ resonance is taken into account only if it is bound or very narrow; otherwise we take a real $\{ip_{1/2}\}$ contour. Another continua, such as $s_{1/2}$, $d_{5/2}, \cdots$, are neglected, as they can be chosen to be real and would only induce a renormalization of the two-body interaction. Altogether, we have 15 $p_{3/2}$ and 14 or 15 $p_{1/2}$ GHF shells in the GSM calculation. Having defined a discretized GHF basis, we construct the many-body Slater determinants from all s.p. basis states (resonant and scattering), keeping only those with at most two particles in the non-resonant continuum. The weight of configurations involving more than two particles in the continuum is usually quite small in the optimal GHF basis.

In the chain of helium isotopes, which are described assuming an inert ^{4}He core, there are only $T = 1$ two-body matrix elements: $(J = 0, T = 1)$ and $(J = 2, T = 1)$. We have adjusted $V_0(J = 0, T = 1)$ to reproduce the experimental g.s. energy of ^{6}He relative to the g.s. of ^{4}He, whereas $V_0(J = 2, T = 1)$ has been fitted to all g.s. energies from ^{7}He to ^{10}He. The adopted values are: $V_0(J = 0, T = 1) = -403\,\mathrm{MeV \cdot fm^3}$ and $V_0(J = 2, T = 1) = -315\,\mathrm{MeV \cdot fm^3}$.

Our previous analysis of $T = 0$ two-body matrix elements in the chain of lithium isotopes suggests that they are gradually reduced with an increasing number of valence neutrons N_n [5]:

$$V_0(J = 1, T = 0) = \alpha_{10}\left[1 - \beta_{10}(N_n - 1)\right],$$
$$V_0(J = 3, T = 0) = \alpha_{30}\left[1 - \beta_{30}(N_n - 1)\right],$$

where $\alpha_{10} = -600\,\mathrm{MeV\,fm^3}$, $\beta_{10} = -50\,\mathrm{MeV\,fm^3}$, $\alpha_{30} = -625\,\mathrm{MeV\,fm^3}$, and $\beta_{30} = -100\,\mathrm{MeV\,fm^3}$. This finding agrees with the conclusion of recent SMEC studies of the binding energy systematics in the *sd*-shell nuclei [12]. In the SMEC, the reduction of the neutron-proton $T = 0$

Table 1. Binding energies of the He isotopes (in MeV) calculated in the GSM using the GHF basis with the M-potential are compared with experimental values.

Nucleus	^{6}He	^{7}He	^{8}He	^{9}He
$\mathcal{B}_{\rm GSM}$ (MeV)	−0.984	−0.475	−3.740	−2.418
$\mathcal{B}_{\rm Exp}$ (MeV)	−0.972	−0.537	−3.112	−1.847

Table 2. The same as in table 1 but for the Li isotopes.

Nucleus	^{6}Li	^{7}Li	^{8}Li	^{9}Li
$\mathcal{B}_{\rm GSM}$ (MeV)	−4.820	−13.008	−15.094	−20.181
$\mathcal{B}_{\rm Exp}$ (MeV)	−3.698	−10.948	−12.981	−17.044

interaction with respect to the neutron-neutron $T = 1$ interaction is associated with a decrease in the one-neutron emission threshold when approaching the neutron drip line, *i.e.*, it is a genuine continuum coupling effect. To account for this effect in the standard Shell Model (SM), one would need to introduce a N-dependence of the $T = 0$ monopole terms which comes about naturally if one includes three-body interactions into the two-body framework of a standard SM [15]. The NN coupling via intermediate scattering states contributes to three-body correlations which are difficult to disentangle from effects generated by the genuine three-body force.

Tables 1 and 2 display binding energies of several He and Li isotopes. The experimental binding energies relative to the ^{4}He core are reproduced fairly well with the SGI interaction. For instance, the g.s. of ^{6}He and ^{8}He are bound, whereas g.s. of ^{5}He and ^{7}He are unbound. Moreover, the so-called *helium anomaly*, *i.e.*, the presence of the higher one- and two-neutron emission thresholds in ^{8}He than in ^{6}He, is well reproduced. Ground-state energies of lithium isotopes relative to the g.s. energy of ^{4}He are described reasonably well, but clearly the particle-number dependence of the matrix elements has to be further investigated in order to achieve a detailed description of the data.

4 Effective interactions in weakly bound systems

In the presence of explicit coupling to the scattering continuum, the treatment of many-body correlations poses a challenge to traditional nuclear structure methods based on SM, and to the derivation of effective interactions in the space of bound states. For weakly bound nuclei, the natural basis for calculating in-medium effective interactions is the complete Berggren basis. The effective interaction consistent with the framework of GSM, depends on the positions of various particle emission thresholds as well as on the distribution and nature of the S-matrix poles.

The genuine features of the continuum coupling correction to the eigenenergy of the closed quantum system near the one-particle emission threshold can be studied in the framework of SMEC. (The description of the SMEC formalism has been given elsewhere [14,2].) In this formalism, the total Hamiltonian $\mathcal{H}$ is divided into the "unperturbed" Hamiltonians H_{QQ} and H_{PP} in the subspaces Q and P of (quasi-)bound (Q subspace) and scattering (P subspace) states, respectively, and the coupling terms H_{QP}, H_{PQ} between these subspaces. The "closed quantum system" approximation is based on replacing $\mathcal{H}$ by H_{QQ} (the standard SM Hamiltonian). In the open quantum formalism, the dynamics in Q subspace is described by an energy-dependent effective Hamiltonian which includes the coupling to the scattering continuum:

$$H^{\rm eff}_{QQ}(E) = H_{QQ} + H_{QP}G^{(+)}_P(E)H_{PQ}\,, \qquad (3)$$

where $G^{(+)}_P(E)$ is a Green's function for the motion of a single nucleon in P subspace. The effective Hamiltonian $H^{\rm eff}_{QQ}$ is a complex-symmetric matrix for E above the particle emission threshold ($E^{(\rm thr)}$), and Hermitian below it. An eigenvalue $\mathcal{E}_i(E) = E_i + E^{(i)}_{\rm corr}$ of $H^{\rm eff}_{QQ}(E)$ can be written as a sum of a closed-system eigenenergy E_i given by H_{QQ} and the correction due to the coupling to the decay channels, which depends on the distance of E_i from the one-particle threshold.

In the one-channel case, and neglecting the off-diagonal terms of $H_{QP}G^{(+)}_P(E)H_{PQ}$, the continuum correction to E_i can be studied analytically assuming a finite-depth, square-well potential for H_{PP} and replacing Q-P couplings by a source term having a radial dependence, which is consistent with the radial dependence of s.p. wave functions which enter in the microscopic calculation of this term [14]. A so-defined model can be rigorously solved [13] to determine basic dependencies of the continuum correction to the eigenenergy of the closed system at the threshold ($E = 0$), as a function of the distance ε of the eigenvalue of H_{PP} (a pole of the S-matrix) from the one-body continuum threshold. In the leading order in ε, one finds:

$$E^{(\ell)}_{\rm corr}(\varepsilon) = -\,{\rm const}\,|\varepsilon|^{-1+\ell/2} + \mathcal{O}\big(|\varepsilon|^0\big), \qquad (4)$$

i.e., the continuum correction at the threshold is singular for $\ell = 0, 1$ states in the limit of $\varepsilon \to 0$, *independently* of whether the considered S-matrix pole is a bound s.p. state, a s.p. resonance or a virtual s.p. state [13]. In general, this behavior leads to the rearrangement of a HF particle vacuum and to the coexistence of two HF minima with different configurations of the S-matrix poles around the threshold. Moreover, the non-perturbative rearrangement of GSM many-body wave functions with a significant $\ell = 0, 1$ s.p. content is expected. Below, we will see an illustration of this genuine behavior in the spectroscopic factor of ^{6}He. The discussion of effects of continuum coupling on spin-orbit splitting in p-shell nuclei can be found in refs. [13,16].

For higher ℓ-values ($\ell \geq 2$), even though the continuum correction is often bigger than for $\ell = 0, 1$ [12], a singular dependence on the position of the S-matrix pole is absent. Therefore, the continuum coupling for high-ℓ orbitals can be mocked up in standard SM calculations by an

adjustment of monopole terms in the effective interaction, in particular, by introducing a suitable particle-number dependence.

5 Spectroscopic factors: example of ^{6}He

As discussed above, the coupling to the particle continuum leads to a strong modification of wave functions in weakly bound/unbound nuclei. A sensitive probe of such modifications is the spectroscopic factor. In this study, we investigate the $p_{3/2}$ spectroscopic factor $S(0^+, p_{3/2})$ for the two lowest 0^+ states of ^{6}He:

$$S\left(0_i^+, p_{3/2}\right) = \Re\left[\sum_k \left(\langle {}^6\mathrm{He}(0_i^+)|\left[|{}^5\mathrm{He}_{\mathrm{g.s.}}\rangle \otimes |p_{3/2}(k)\rangle\right]_{J=0}\right)^2\right], \quad (5)$$

where $i = 1, 2$ and the sum runs over all $|p_{3/2}(k)\rangle$ states, *i.e.*, both the $0p_{3/2}$ pole and the non-resonant $p_{3/2}$ continuum. (It is to be noted that the Gamow states are normalized using the squared wave function and not the modulus of the squared wave function.) The spectroscopic factors are very sensitive to discretization effects. Below, we take 26 points for the $p_{3/2}$ contour, and 14 points for the $p_{1/2}$ complex contour. The $0p_{1/2}$ resonant state has to be included, as the 0_2^+ state of ^{6}He in the pole approximation is built from two neutrons in $0p_{1/2}$.

In the quasi-stationary approach with Gamow states, the spectroscopic factor (5) is, in general, complex. An interpretation of these complex values has been given by Berggren [17]: the real part of the matrix element can be associated with the average value, while the imaginary part represents the uncertainty of the mean value. Therefore, if the overlap matrix element has a large imaginary value, the spectroscopic factor can become negative.

Figure 1 shows the spectroscopic factor of the ^{6}He g.s. in the $[|{}^5\mathrm{He}\rangle \otimes |p_{3/2}\rangle]_0$ channel as a function of the position of the $0p_{3/2}$ pole of the S-matrix in ^{5}He. (The energy of the $0p_{3/2}$ pole is varied by changing the depth of the central part of the WS potential.) The results of the full GSM calculations in the model space, which includes $0p_{3/2}$, $0p_{1/2}$ s.p. resonances and the states of the discretized complex continuum, exhibit an intricate dependence on the position of the $0p_{3/2}$ pole. If the $0p_{3/2}$ s.p. state of ^{5}He is bound, the spectroscopic factor decreases smoothly when $0p_{3/2}$ approaches the continuum threshold. At the threshold, where the coupling to the non-resonant continuum is strongest, the spectroscopic factor reaches its lowest value. The behavior of the spectroscopic factor changes dramatically if $0p_{3/2}$ becomes a resonance, as it grows with increasing energy of the $0p_{3/2}$ state. This is an illustration of how strongly the analytic features of the S-matrix may influence the spectroscopic observables in a weakly bound system.

The role of the completeness of the s.p. basis can be assessed by comparing results of the full GSM calculation

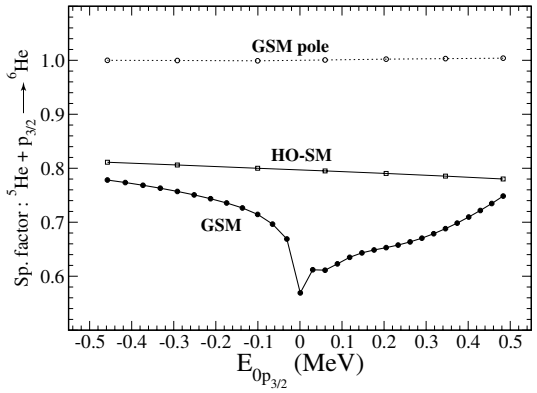

Fig. 1. Spectroscopic factor of the ^{6}He ground state in the $[|{}^5\mathrm{He}\rangle \otimes |p_{3/2}\rangle]_0$ channel as a function of the energy of the $0p_{3/2}$ s.p. state in ^{5}He. Thick solid line: GSM results; thin solid line: the equivalent SM results in the HO-SM approximation; dashed line: restricted GSM calculations in the pole approximation, *i.e.*, including resonances $0p_{3/2}$ and $0p_{1/2}$ only.

with the results obtained in the pole approximation (pole-GSM), where the basis states of the non-resonant continuum are neglected. In the latter case, the spectroscopic factor changes smoothly with the energy of the $0p_{3/2}$ state. This clearly demonstrates that the complicated dependence of the spectroscopic factor found in GSM is the result of an interplay between discrete states and the non-resonant continuum states in the many-body wave function of ^{6}He.

To compare the GSM results with the results of the standard SM procedure, we performed calculations in the harmonic oscillator basis. The s.p. energies in such "equivalent SM calculations" (HO-SM approximation) are given by the real parts of $0p_{1/2}$ and $0p_{3/2}$ eigenvalues of the WS potential generating the GSM basis. Such equivalent SM calculation yields, as expected, a smooth and monotonic energy variation of the spectroscopic factor. The GSM results are close to the HO-SM results for well bound $0p_{3/2}$ s.p. state, *i.e.*, when the coupling to the non-resonant continuum states is weak. On the contrary, the difference between GSM and HO-SM is strongest if the $0p_{3/2}$ pole lies at the threshold.

It is worth noting that there is a significant difference between the results of HO-SM and pole-GSM calculations. In both cases, the dimension of the model space is identical but the radial wave functions used to calculate the matrix elements of the two-body Hamiltonian are different. In particular, the $0p_{1/2}$ s.p. state is a broad resonance in GSM, and the matrix elements of the SGI interaction involving this state are noticeably reduced as compared to the HO-SM variant. Consequently, the configuration mixing in the $(0p_{3/2}0p_{1/2})$ space is stronger in HO-SM.

Figure 2 shows the spectroscopic factor (5) for the first excited 0_2^+ state of ^{6}He. There are only two 0^+ states in the $(0p_{3/2}0p_{1/2})$ model space of HO-SM and pole-GSM; hence the results of figs. 1 and 2 are strongly correlated. (The sum of both spectroscopic factors is equal to one.) A small value of the spectroscopic factor in GSM cannot

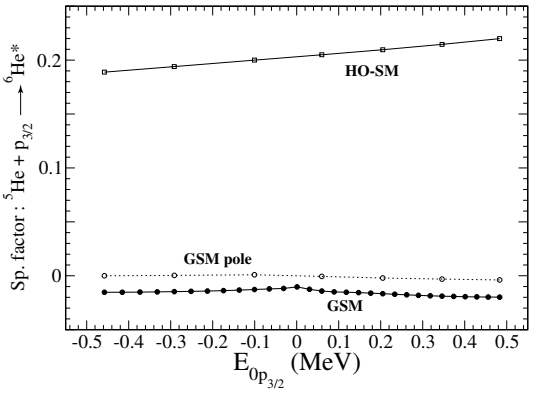

Fig. 2. The same as in fig. 1 except for the second 0^+ excited state of the ^{6}He.

be explained in the same way. In fact, the configurations involving a $0p_{3/2}$ s.p. state (bound or resonance) are spread over a huge number of excited 0^+ states, all of them unbound, having a dominant contribution from the non-resonant continuum basis states. Consequently, the spectroscopic factor is mainly concentrated in a single state, the g.s. of ^{6}He in the present case, and other 0^+ states have negligibly small amplitudes. For the bound $0p_{3/2}$ s.p. state, the maximum value of the spectroscopic factor in the distribution over all 0^+ states decreases when $0p_{3/2}$ approaches the continuum threshold.

The mechanism of concentration of the spectroscopic factor in a single state discussed in this section is a genuine effect of the strong coupling to the continuum. Going away from the valley of stability towards drip lines, one should expect to see a gradual reduction of the spreading of spectroscopic factors over different J^π, T states, which is characteristic of the gradual evolution of correlations in the many-body system due to the enhanced continuum coupling. Obviously, the description of such an evolution is beyond the scope of the standard SM.

6 Application of the density matrix renormalization group techniques for solving the GSM problem

The complex Berggren ensemble of the GSM contains many states representing a discretized non-resonant continuum. Consequently, the dimension of the (non-Hermitian) GSM Hamiltonian matrix grows extremely fast with the number of active shells, and this "explosive" growth is much more severe than in the standard SM which deals with the pole space only. In practice, most of the configurations involving many nucleons in the non-resonant continuum contribute very little to wave functions of low-energy physical states which are dominated by the pole space configurations and by configurations with a small number of nucleons in the non-resonant states in the neighborhood of these pole states. This feature of GSM calls for a development of a procedure for selecting the most important configurations involving continuum states. A promising approach is the DMRG method developed originally in the context of quantum lattices [18] and recently applied to SM problems with schematic Hamiltonians [19]. The main idea is to gradually consider different s.p. shells in the configuration space and retain only $N_{\rm opt}$ the most optimal states dictated by the one-body density matrix. Below, we shall discuss the application of the DMRG method to the g.s. configuration of ^{6}He in GSM. In this case, the configuration space is divided into two subspaces: A (s.p. resonances $0p_\alpha$, $\alpha = 1/2, 3/2$) and B (s.p. states/shells representing the non-resonant continua $\{p_\alpha\}$, $\alpha = 1/2, 3/2$). In the initial phase (*the warm-up phase*), one calculates and stores all the possible matrix elements of suboperators of the Hamiltonian in A:

$$a^\dagger, \left(a^\dagger \widetilde{a}\right)^K, \left(a^\dagger a^\dagger\right)^K, \left(\left(a^\dagger a^\dagger\right)^K \widetilde{a}\right)^L, \left(\left(a^\dagger a^\dagger\right)^K \left(\widetilde{a}\widetilde{a}\right)^K\right),$$

and constructs all the states $|k\rangle$ with 0, 1, 2 particles coupled to all possible j-values. Then, from each continuum $\{p_\alpha\}$, one picks up a s.p. state, calculates for this added pair of shells the matrix elements of suboperators, and constructs all the states $|i\rangle$ with 0, 1, 2 particles coupled to all possible j-values. In the following, one adds "one by one" pairs of s.p. states in B and repeats the procedure until the number of states $|i\rangle$ is larger than $N_{\rm opt}$. Then the Hamiltonian is diagonalized in the space $\{|k\rangle_A |i\rangle_B\}^J$ made of vectors in A and B. Obviously, the number of particles in such states is equal to the total number of valence particles, and J is equal to the angular momentum of the state of interest ($J = 0$). From the eigenstates

$$|\Psi\rangle = \sum c_{ki} \{|k\rangle_A |i\rangle_B\}^J, \tag{6}$$

one calculates the one-body density matrix,

$$\rho^B_{ii'} = \sum_k c_{ki} c_{ki'}, \tag{7}$$

in different blocks with a fixed value of j in states $|i\rangle$, $|i'\rangle$. The density matrix is then blockwise diagonalized and $N_{\rm opt}$ eigenstates $|u_\nu\rangle$ having the largest eigenvalues ω^B_ν are retained. (In GSM, eigenvalues of the density matrix are complex and the eigenstates of ρ^B are selected according to the largest absolute value of the density eigenvalues.) Those eigenvalues correspond to the most important states of the enlarged set. All the matrix elements of suboperators for the optimized states are recalculated; they are linear combinations of previously calculated matrix elements. Then, the next pair of non-resonant continuum states is added and, again, only the $N_{\rm opt}$ states are kept. This procedure is repeated until the last shell in B is reached, providing a "first guess" for the wave function of the system.

This ends a warm-up phase, and a *sweeping phase* begins. At this point, one constructs states with 0, 1, 2 particles and then the process continues in the reverse direction until the number of vectors becomes larger than $N_{\rm opt}$. If the m-th shell in B is reached, the Hamiltonian is diagonalized in the set of vectors: $\{|k, i_{\rm prev}\rangle |i\rangle\}^J$, where $i_{\rm prev}$ is a previously optimized state (first $m-1$ p-shells in B),

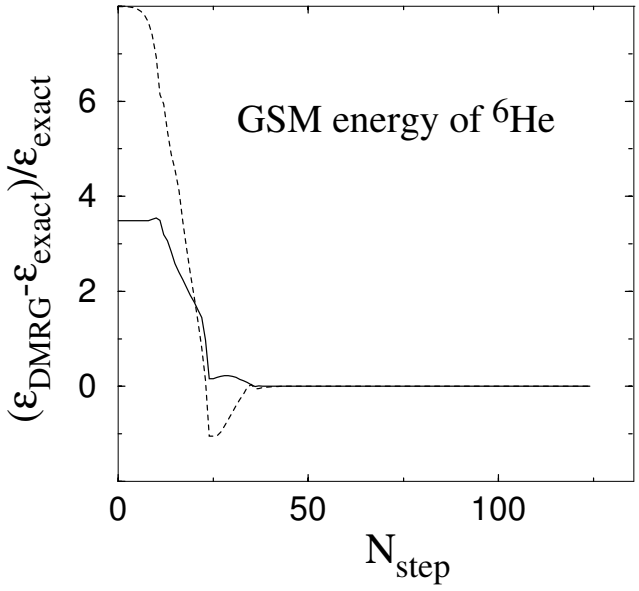

Fig. 3. The relative difference between the exact g.s. GSM energy of ^{6}He ($\varepsilon_{\rm exact}$) and the energy of this state calculated in GSM + DMRG approach ($\varepsilon_{\rm DMRG}$) as a function of the number of iteration steps. Solid (dashed) line marks the real (imaginary) part of the GSM + DMRG energy. See text for details.

and i is a new state ($i > m$). The density matrix is then diagonalized and the $N_{\rm opt}$ i-states are kept. The procedure continues by adding the $(m-1)$-th pair of shells, etc., until the first state in B is reached. Then the procedure is reversed again: the first pair of shells is added, then the second, the third, etc. The succession of sweeps is successful if the energy converges.

Figure 3 illustrates the convergence of real and imaginary parts of the g.s. energy of ^{6}He calculated in the DMRG procedure as a function of the number of steps, $N_{\rm step}$. In this example, the number of shells included in blocks A and B are 2 and 50, respectively. At each step we keep $N_{\rm opt} = 6$ states. For these parameters, the warm-up phase is completed in 25 steps, and fully converged GSM + DMRG results are found in 15 steps, *i.e.* in less than one sweep. This example demonstrates that a finite-system algorithm of DMRG is very efficient in selecting the most important GSM continuum configurations. In the considered example, a total dimension D of the GSM Hamiltonian is 702, and the rank of the biggest matrix to be diagonalized in GSM + DMRG is $d = 32$. The gain factor D/d grows very fast with the number of valence particles and with the number of shells in the non-resonant continuum (B block).

7 Conclusion

Coupling to the non-resonant continuum and the multi-configuration mixing can be consistently described in the framework of the GSM. The explosive growth of dimensionality in GSM, associated with the inclusion of a large number of states in the non-resonant continuum, can be strongly reduced by applying techniques of the DMRG in solving the GSM problem. The novel feature of GSM, absent in the standard SM, is a strong influence of S-matrix poles on the weakly bound/unbound many-body states. For the low-ℓ orbits ($\ell = 0, 1$), the continuum coupling may induce the instability of the HF vacuum and non-perturbative rearrangement of the wave function. We have demonstrated that this effect can be seen in the properties of spectroscopic factors. A similar mechanism may also influence the spin-orbit effects, pair-transfer amplitudes, nuclear collectivity, and properties of nuclear excitations. Further systematic investigations of weakly bound nuclei, both experimentally and theoretically, will undoubtedly shed new light on the salient features of the continuum coupling and will identify the most pertinent observables affected by a gradual appearance of open channels when moving towards particle drip lines.

This work was supported in part by the U.S. Department of Energy under Contracts Nos. DE-FG02-96ER40963 (University of Tennessee), DE-AC05-00OR22725 with UT-Battelle, LLC (Oak Ridge National Laboratory), and DE-FG05-87ER40361 (Joint Institute for Heavy Ion Research).

References

1. J. Dobaczewski, W. Nazarewicz, Philos. Trans. R. Soc. London, Ser. A **356**, 2007 (1998).
2. J. Okołowicz, M. Płoszajczak, I. Rotter, Phys. Rep. **374**, 271 (2003).
3. N. Michel, W. Nazarewicz, M. Płoszajczak, K. Bennaceur, Phys. Rev. Lett. **89**, 042502 (2002).
4. N. Michel, W. Nazarewicz, M. Płoszajczak, J. Okołowicz, Phys. Rev. C **67**, 054311 (2003).
5. N. Michel, W. Nazarewicz, M. Płoszajczak, Phys. Rev. C **70**, 064313 (2004).
6. N. Michel, W. Nazarewicz, M. Płoszajczak, J. Okołowicz, J. Rotureau, Acta Phys. Pol. B **35**, 1249 (2004).
7. N. Michel, W. Nazarewicz, M. Płoszajczak, J. Rotureau, arXiv:nucl-th/0401036.
8. R.I. Betan, R.J. Liotta, N. Sandulescu, T. Vertse, Phys. Rev. Lett. **89**, 042501 (2002).
9. R.I. Betan, R.J. Liotta, N. Sandulescu, T. Vertse, Phys. Rev. C **67**, 014322 (2003).
10. T. Berggren, Nucl. Phys. A **109**, 265 (1968).
11. G. Hagen, M. Hjorth-Jensen, J.S. Vaagen, arXiv:nucl-th/0410114.
12. Y. Luo, J. Okołowicz, M. Płoszajczak, N. Michel, arXiv:nucl-th/0201073.
13. N. Michel, W. Nazarewicz, J. Okołowicz, M. Płoszajczak, *Proceedings of the International Nuclear Physics Conference (INPC 2004)*, (Elsevier B.V., Amsterdam, 2005).
14. K. Bennaceur, F. Nowacki, J. Okołowicz, M. Płoszajczak, Nucl. Phys. A **651**, 289 (1999); **671** (2000) 203.
15. A. Zuker, Phys. Rev. Lett. **90**, 042502 (2003).
16. N. Michel, W. Nazarewicz, M. Płoszajczak, these proceedings.
17. T. Berggren, Phys. Lett. B **373**, 1 (1996).
18. S.R. White, Phys. Rev. B **48**, 10345 (1993).
19. J. Dukelsky, S. Pittel, S.S. Dimitrova, M.V. Stoitsov, Phys. Rev. C **65**, 054319 (2002).